COMMUNICATION

Expanding the Variety of Zirconium-based Inorganic Building Units for Metal-organic Frameworks

Sebastian Leubner[a], Haishuang Zhao[b], Niels Van Velthoven[c], Mickaël Henrion[c], Helge Reinsch[a], Dirk E. De Vos*[c], Ute Kolb*[b], Norbert Stock*[a]

Abstract: Two new zirconium based metal-organic frameworks with the composition $[Zr_6O_4(OH)_4(OAc)_6(BDC)_3]$ (CAU-26) and $[Zr_5O_4(OH)_4(OAc)_4(BDC)_2]$ (CAU-27) are reported, which were synthesized from acetic acid, a rarely utilized but green and sustainable solvent (BDC^{2-}: 1,4-benzenedicarboxylate). Structure determination aided by automated electron diffraction tomography revealed that CAU-26 is composed of layers of well-known $\{Zr_6O_8\}$ clusters interconnected by terephthalate ions. In contrast CAU-27 exhibits a three dimensional structure with a so far unknown type of one-dimensional inorganic building unit (IBU), which can be rationalized as condensed polyhedron-sharing chains of $\{Zr_6O_8\}$ clusters. CAU-26 occurs as an intermediate of the CAU-27 synthesis and can be isolated easily, when reaction temperature and time are decreased. We were also able to synthesize two isoreticular derivatives of CAU-27 with extended linker molecules by implementing 4,4'-biphenyldicarboxylic acid (BPDC) and 5,5'-dicarboxy-2,2'-bipyridine (BIPY). All materials show high thermal and chemical stability as well as permanent microporosity. The excellent stability of CAU-27-BIPY was exploited to synthesize a performant iridium-supported heterogeneous MOF-based catalyst for the direct C-H borylation of arenes.

Introduction: Zirconium based metal-organic frameworks (MOFs) represent probably one of the most well studied group of materials in MOF chemistry, owing to their high thermal, chemical and mechanical stability[1] combined with low toxicity[2] and high availability/low price of zirconium itself. The stability originates from the strong coordination bond between highly charged Zr^{4+} ions (strong Lewis acids) and oxygen anions from the ligand molecules (strong Lewis bases) and is in agreement with the HSAB (hard and soft acids and bases) principle.[3] In general high stability and surface areas of MOFs are desirable for potential applications like catalysis, gas storage, heat transformation and medical uses.[4] However, a major drawback is given by the synthesis conditions of zirconium MOFs, since the majority of reaction routes utilize the highly carcinogenic solvent *N,N*-dimethylformamide (DMF), which tends to decompose under hydrolysis of the amide bond at elevated temperatures or in an catalytic environment (e.g. acids, bases, metal ions).[5] As a consequence, a small number of water based routes has been developed, which gave access to DMF free syntheses of functionalized UiO-66 derivatives[6] or Zr fumarate (MOF-801)[7], to name just some of the most prominent examples. In recent years our group, together with cooperation partners, pushed these developments further by discovering multiple water based synthesis routes for existing, but also completely new MOFs.[8-12]

As stated by Bai *et al*. in 2016 only very few inorganic building units (IBUs) are known for zirconium and the very similar hafnium MOFs. The by far most frequently observed IBU is the $\{Zr_6O_8\}$ cluster.[13-16] Molecular clusters of this composition have been intensively studied in the past and many supramolecular structures have emerged just recently.[17-21] More complex clusters have been also reported for MOFs. Cliffe *et al.* for example described triply edge-sharing dimers of $\{Hf_6O_8\}$ clusters in a linker defective layered UiO-67 analogue[22], while our group discovered a new chain type IBU in the MOF CAU-22[10], which is composed of hexagonally arranged μ-OH bridged $\{Zr_6O_8\}$ clusters which are interconnected by 2,5-pyrazinedicarboxylate ions. A different and less frequently observed IBU is represented by the 1D chain of {ZrO} polyhedra within the MIL-140 series.[23]

For MOF structure determination single crystal X-ray analysis is the most straightforward way and therefore usually the method of choice. Unfortunately zirconium MOFs tend to form fine microcrystalline powders, the characterization of which is challenging and requires advanced state of the art tools like electron diffraction and sophisticated structure determination from powder X-ray diffraction (PXRD) data combined with RIETVELD refinements. Automated electron diffraction tomography (ADT)[24,25], developed around ten years ago, delivers three-dimensional electron diffraction data from single nanocrystals, using a transmission electron microscope (TEM). In the last decade, electron crystallography has shown its power and successful applications in structure analysis of nanocrystalline materials with challenging structural features[26-32] like extra-large lattice parameters, disorder, pseudo-symmetry, small crystalline domains, multiple phases and detection of light scattering atoms (e.g. Li, B, H). The quality of the extracted reflection intensities can be increased by coupling ADT with precession electron diffraction (PED).[33]

One of the main interests of stable, large pore MOFs is that they are flexible platforms for the immobilization of precious homogeneous metal catalysts. This is especially relevant in the rich domain of C-H activation catalysis, with formation of e.g. C-C, C-N or C-B bonds. Arylboronic acids are very important intermediates in organic synthesis that can be used in a plethora

[a] MSc. S. Leubner, Dr. H. Reinsch, Prof. Dr. N. Stock
Institute for Inorganic Chemistry
University of Kiel
Max-Eyth Straße 2, 24118 Kiel, Germany.
E-mail: stock@ac.uni-kiel.de
[b] MSc. H. Zhao, Prof. Dr. U. Kolb
Institute of Inorganic Chemistry and Analytical Chemistry
Johannes-Gutenberg-University of Mainz
Duesbergweg 10-14, 55128 Mainz, Germany.
[c] Ir. N. Van Velthoven, Dr. M. Henrion, Prof. Dr. D. De Vos
Centre for Membrane Separations, Adsorption, Catalysis and Spectroscopy for Sustainable Solutions (cMACS)
KU Leuven Celestijnenlaan 200F, 3001 Leuven (Belgium)

Supporting information for this article is given via a link at the end of the document.

of synthetic procedures. Among the different routes to synthesize arylboronic acids, direct C-H borylation of arenes using bis(pinacolato)diboron (B_2pin_2) is the most environmentally benign process, which can be efficiently catalysed by homogeneous iridium complexes. However, these homogeneous iridium complexes are expensive and very difficult to recover and recycle, highlighting the need for stable, heterogeneous iridium catalysts. Zirconium MOFs with high chemical and thermal stability represent a class of support materials that could be appropriate to address these problems.

Here we report the results of our detailed investigation on the use of the uncommon green and sustainable solvent acetic acid for MOF synthesis, which lead to the discovery of two new zirconium MOFs (CAU-26 & CAU-27). The crystal structure of CAU-27 exhibits a new IBU of highly condensed, zirconium sharing chains of the well-known $\{Zr_6O_8\}$ cluster. For structure and property determination, both materials were comprehensively characterized by electron and X-ray diffraction as well as many other supporting techniques. Furthermore, a functionalized derivative of CAU-27 (CAU-27-BIPY) was prepared as an iridium-loaded heterogeneous catalyst and tested for the direct C-H borylation of arenes.

Results & Discussion: Our investigation of green and sustainable solvents for the synthesis of Zr-MOFs led to the discovery of two new crystalline compounds (denoted as CAU-26 and CAU-27-BDC) upon reacting terephthalic acid (H_2BDC) and zirconium acetate in pure acetic acid under solvothermal conditions. After 24 hours at a temperature of 160 °C CAU-26 is obtained, while using the same molar ratios of starting materials with increased reaction time and temperature (10 days, 220 °C) leads to the formation of CAU-27-BDC (Fig. S1 and S3). Reactions at 220 °C with decreased reaction times further revealed, that CAU-26 occurs as an intermediate in the CAU-27-BDC synthesis, which is very slowly but fully transformed to CAU-27-BDC. The slow rate of this transformation demonstrates that CAU-27-BDC is the thermodynamically favored product, while CAU-26 is only kinetically stable. After thorough purification the compounds were comprehensively characterized by electron and X-ray powder diffraction, gas adsorption, infrared (IR), RAMAN and ^{1}H NMR spectroscopy as well as thermogravimetric (TG) and elemental analyses (EA) in order to determine their structures and chemical compositions (data provided in the SI). It should be noted, that the purification process for CAU-27 comprises two steps. The first step involves treatment with DMF and the second step utilizes DMF/HCl mixtures (adapted procedure by Feng *et al.*[34]). The latter leads to partial exchange of acetate with formate ligands. As shown in Fig. S9, CAU-26 consists mainly of low crystalline agglomerated particles. Nevertheless, some higher quality crystals with a plate-like morphology were investigated. The material is electron beam sensitive, thus, during ADT measurements, MOF materials were cooled down and kept at liquid nitrogen temperature with a cryotransfer TEM holder to reduce beam damage. For structure elucidation of CAU-26 via ADT two independent plate-like crystals were chosen, one lying and another standing upright (Fig. S10). The reconstruction of 3D diffraction volumes delivered a primitive hexagonal lattice for CAU-26 (Fig. S1, Tab. S2-3). Strong diffuse scattering effects are visible along the *c** axis, indicating a stacking disorder along the *c* axis. No systematic extinction could be observed. Poor crystallinity (achievable resolution of 1.3 Å) and strong diffuse scattering prevented a complete structure determination from ADT data. Only in the case of space group *P*3*m*1 (No. 156), the structure solution resulted in reasonable Zr positions, which could be used to construct the $\{Zr_6O_8\}$ cluster. With the information of the cluster positions, the space group and the stacking disorder it was possible to construct a structural model with force field methods, showing that CAU-26 consists of two-dimensional layers of six-connected $\{Zr_6O_8\}$ clusters (Fig. 1).

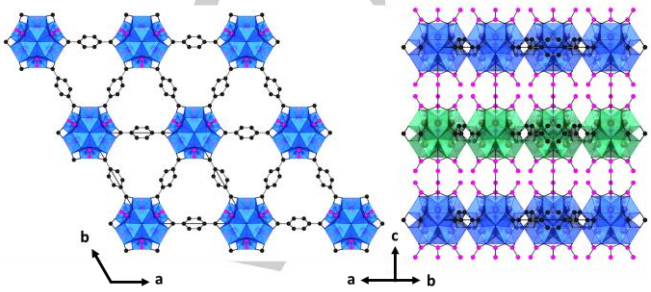

Figure 1. Structure representation of CAU-26 with layers composed of $\{Zr_6O_8\}$ clusters, which are interconnected to six other clusters by BDC^{2-} ions (left) and stacking of the layers (right). Carbon atoms of the BDC^{2-} and acetate ions are displayed in black and pink, respectively and layers are displayed in blue and green for clarity. Zirconium: bronze, oxygen: red, carbon: black, hydrogen: not displayed, $\{Zr_6O_8\}$ cluster: blue.

In this model each carboxylate group of a terephthalate ion is coordinating to two Zr^{4+} ions of a cluster in a corner-to-corner bridging manner. The six remaining coordination sites of the cluster located above and below the linker plane are most likely capped by acetate ligands, which were available in high excess during the synthesis. This structure model corresponds to a MOF with the formula $[Zr_6O_4(OH)_4(OAc)_6(BDC)_3]$. However, based on the compositional data, CAU-26 seems to exhibit cluster and/or linker defects, which would be in line with its low crystallinity and with differing cluster occupancies of the layers. A detailed structure description and compositional analysis is given in the supporting information.

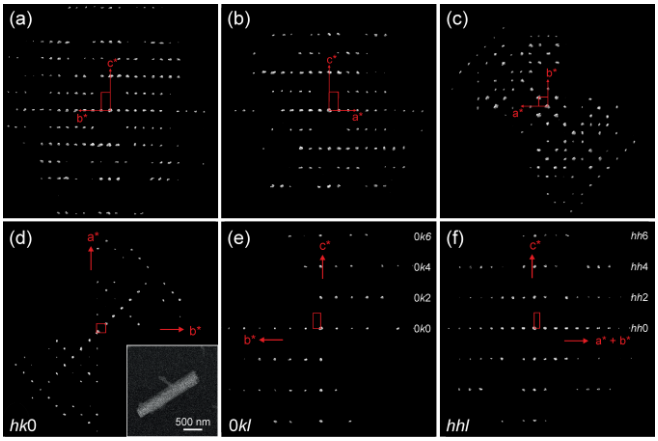

Figure 2. Reconstructed 3D diffraction volumes of CAU-27-BDC obtained from ADT data viewed down the three main axis (a - c). 2D slices cut from reconstructed 3D reciprocal space corresponding to 0*kl* (d), *h*0*l* (e) and *hhl* (f) planes. The crystal selected for the acquisition of ADT data is shown as an inset in (d).

For the structure determination of CAU-27-BDC a mildly purified sample (step 1, see SI 2.4) was used. The structure was determined by ADT and also by direct methods from PXRD data and was confirmed by RIETVELD refinement. CAU-27-BDC consists of needle-like crystals which are slightly less sensitive towards electron radiation than CAU-26. A tetragonal unit cell was obtained from the reconstructed ADT data taken from an approximately 200 nm thick rod of CAU-27-BDC (Fig. 2/Fig. S11, Tab. S2-3). Symmetry analysis from three major zones (Fig. 2/Fig. S11) results in the extinction symbol *I* — *c* — with three possible space groups: *I*4*cm* (No. 108), *I*4*c*2 (No. 120) or *I*4/*mcm* (No. 140). The *ab initio* structure solution of CAU-27-BDC was successfully performed in the space group *I*4/*mcm* with direct methods from ADT data with 1.0 Å resolution and delivered a meaningful structure model and a well-resolved Fourier potential map (Fig. 3).

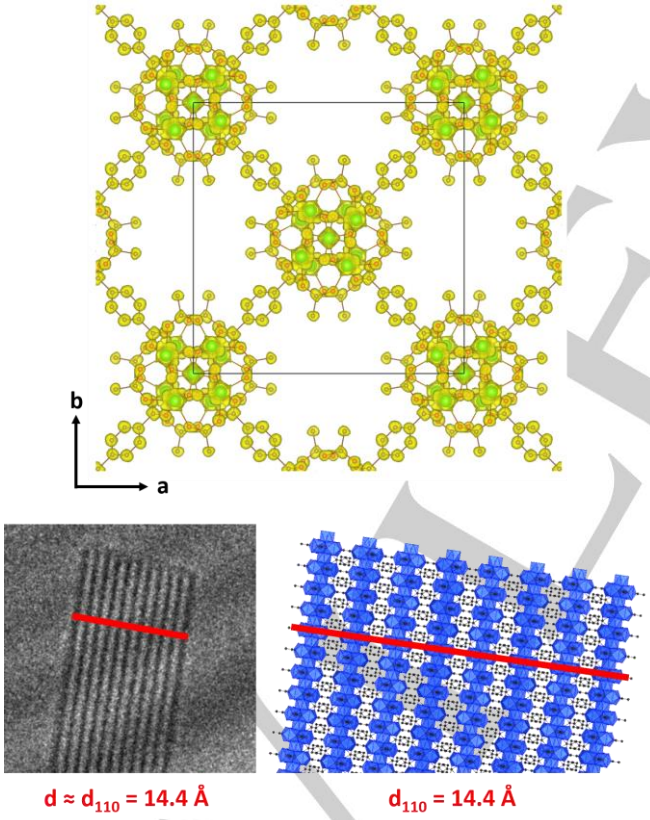

Figure 3. Fourier potential map of CAU-27-BDC derived from ADT data overlaid with the atomic framework model viewed along [001] (top) and a HRTEM image viewed along [110] (bottom left) with a representation of the crystal structure (bottom right). Zr-O IBU: blue.

The crystal structure was refined by the RIETVELD method from PXRD data (Fig. S20, Tab. S5). Crystallographic data for the structural analyses have been deposited with the Cambridge Crystallographic Data Centre (CCDC numbers 1880628-1880629). CAU-27-BDC consists of infinite chains of condensed ZrO_8 polyhedron-sharing $\{Zr_6O_8\}$ clusters, which are interconnected by terephthalate ions in two dimensions. This leads to the formation of one-dimensional channels running parallel to the IBUs within the structure (Fig. 4). Four remaining coordination sites per cluster are capped by acetate ligands, giving an overall formula of $[Zr_5O_4(OH)_4(OAc)_4(BDC)_2]$. High-resolution transmission electron microscopy (HRTEM) was carried out to observe the real space atomic structure information of CAU-27-BDC. HRTEM images viewed along [010] (Fig. 3, Fig. S12) are in excellent agreement with the backbone constituted from $\{Zr_6O_8\}$-clusters running along the *c* axis, further confirming the crystal structure.

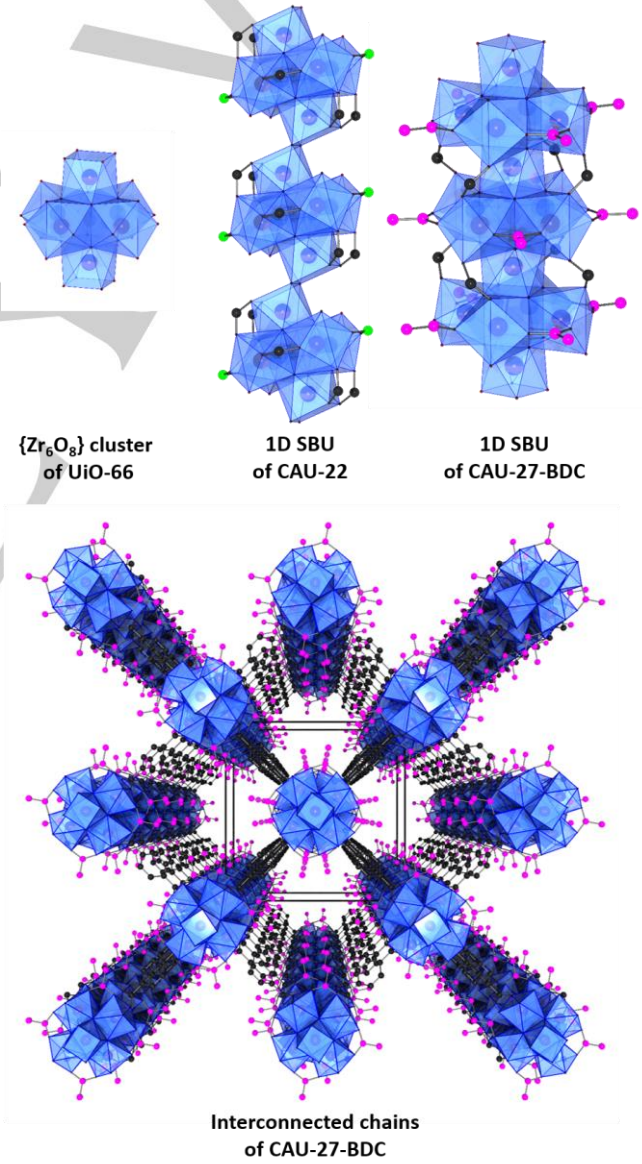

Figure 4. Structural components of CAU-27-BDC including the $\{Zr_6O_8\}$ cluster (top left), the IBU in comparison with the IBU of CAU-22 (top right and middle)

and the interconnected chain motive (bottom). Formate carbon atoms of CAU-22 are displayed in green and acetate carbon atoms of CAU-27-BDC are displayed in pink for clarity. Zirconium: bronze, oxygen: red, carbon: black, hydrogen: not displayed, Zr-O IBU: blue.

The concept of isoreticular expansion[35] can be applied to CAU-27-BDC, if terephthalic acid as starting material is replaced by 4,4'-biphenyldicarboxylic acid (H_2BPDC) or 5,5'-dicarboxy-2,2'-bipyridine (H_2BIPY) under otherwise analogous synthesis conditions. In this case isoreticular derivatives with a larger pore channel diameter than CAU-27-BDC (7 Å), denoted as CAU-27-BPDC (13 Å) and CAU-27-BIPY (13 Å), are obtained (Fig. 5). The structure of CAU-27-BPDC could be also confirmed by RIETVELD methods (Fig. S21, Tab. S5). Subsequently a LEBAIL fit was sufficient to confirm phase purity of CAU-27-BIPY (Fig. S22, Tab. S5). During the formation of these derivatives, no CAU-26-like intermediate could be isolated, indicating that a possible intermediate is rather too short-living or simply not occurring in the crystallization process. We assume that this behavior could be related to the lower solubility of the extended linker molecules in acetic acid.

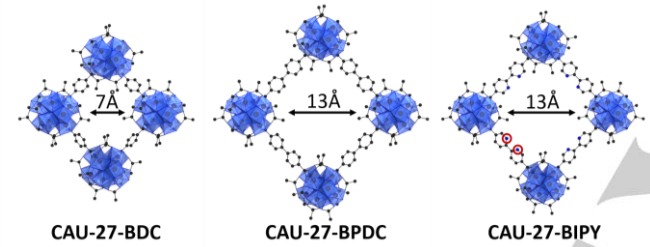

Figure 5. Different diameters of the one dimensional channels within the CAU-27 series. Nitrogen atoms of CAU-27-BIPY are displayed in blue and highlighted by red circles. Zirconium: bronze, oxygen: red, carbon: black, hydrogen: not displayed, Zr-O IBU: blue.

Nitrogen adsorption measurements were carried out to determine the specific BET surface areas and micropore volumes (Tab. 1, Fig. S40-43) of CAU-26 and the series of CAU-27 MOFs. Further, water adsorption properties were investigated, showing that all materials adsorb significant amounts of water (Fig. S44-47).

Table 1. BET surface areas and micropore volumes of CAU-26 and CAU-27-BDC as well as its derivatives in comparison with theoretical values. All samples were activated at two different temperatures for 24 h under reduced pressure, before nitrogen adsorption measurements were carried out, in order to observe the effect of acetate/formate removal. Theoretical values were only calculated for CAU-27 compounds containing coordinated acetate ligands.

Name	Theo. BET surface [m^2/g]	Theo. micropore volume [cm^3/g]	Exp. BET surface [m^2/g]	Exp. micropore volume [cm^3/g]
CAU-26	-	-	827/779[a]	0.35/0.34[a]
CAU-27-BDC	370	0.13	264/360[b]	0.13/0.16[b]
CAU-27-BPDC	905	0.37	577/578[b]	0.27/0.26[b]
CAU-27-BIPY	905	0.37	421/561[b]	0.21/0.24[b]

[a] Left value: activation at 150 °C. Right value: activation at 280 °C.

[b] Left value: activation at 160 °C. Right value: activation at 320 °C.

The surface area of CAU-26 is slightly lower after activation at 280 °C compared to activation at 150 °C. This difference is within the error margin of the method, but it is also reproducible. It can be explained by the removal of acetate ligands at high temperatures, which causes a reduction of the interlayer distances within the structure (Fig. S1,S2). This explanation is also in line with the results of other characterization methods (TG, EA, IR, ^{1}H NMR). The surface areas of the CAU-27 MOFs after an activation at 160 °C are smaller than the theoretical values. We consider this behaviour as reasonable for needle shaped crystals, since agglomeration of particles or single defects (e.g. terephthalate ligand at an acetate coordination site) can lead to blocking of whole pore channels.

Activation at 320 °C leads to removal of acetate/formate ions and accordingly to structural changes, which are clearly visible in the PXRD and spectroscopic data as well as the thermogravimetric and CHN analysis. These results are further discussed in the SI.

Chemical and thermal stability tests have also been carried out. The results from TG (Fig. S23-30) and variable temperature diffraction experiments (Fig. S32-39) prove the high thermal stability of the new MOFs (~ 400 - 470°C) considering the phase transition upon acetate/formate removal as non-destructive. Furthermore 24 hour stability tests within various different solvents and aqueous solutions across a large pH range (1-12) also showed that all materials exhibit outstanding chemical stability, especially towards acids (stable in a pH range of at least 1-11) and common organic liquids (Tab. S14).

Given its high chemical and thermal stability, CAU-27-BIPY was loaded with $[Ir(COD)(OMe)]_2$ (COD: 1,5-cyclooctadiene) via postsynthetic metalation (supporting information) and applied as single-site heterogeneous catalyst for the direct C-H borylation of arenes. The iridium-loaded CAU-27 material (CAU-27-BIPY-Ir) was able to efficiently transform arenes possessing a variety of functional groups, affording the borylated products in excellent yields and in similar selectivities as stated in the literature (Table 2).

Table 2. Direct C-H borylation of arenes catalysed by CAU-27-BIPY-Ir.[a]

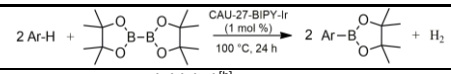

Entry	Substrate	Product	yield (%)[b] (*o*:*m*:*p*)	Entry	Substrate	Product	yield (%)[b] (*o*:*m*:*p*)
1			82 (*0:64:36*)	5		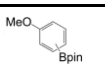	92 (*0:72:28*)
2			82	6		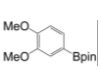	85
3			74				
4			56	7			83

[a] All reactions were conducted under neat conditions with 0.118 mmol B_2pin_2, 1.250 ml arene, 1 mol % CAU-27-BIPY-Ir at 100 °C for 24 h.

[b] Yields and isomer ratios determined by GC analyis.

As a reference, the well-known UiO-67-BIPY MOF, consisting of 5,5'-dicarboxy-2,2'-bipyridine linkers was synthesized and loaded with iridium in a similar way as CAU-27-BIPY. Although a slightly higher yield was obtained for the direct C-H borylation of toluene with UiO-67-BIPY-Ir compared to CAU-27-BIPY-Ir in the first run, significantly lower yields were obtained with UiO-67-BIPY-Ir in the second and third run (Table 3). The heterogeneity of both systems was verified by performing hot filtration experiments (Figures S64-65), indicating that the less efficient recycling of UiO-67-BIPY-Ir compared to CAU-27-BIPY-Ir is presumably due to pore blockage and framework collapse. Indeed, PXRD analysis of the materials after reaction revealed that UiO-67-BIPY-Ir lost most of its long-range order while the structure of CAU-27-BIPY was well preserved after the catalytic reactions (Figures S66-67).

Table 3. Recycling tests of CAU-27-BIPY-Ir and UiO-67-BIPY-Ir.[a]

Run	Ir-catalyst	yield (%)[b]
1	CAU-27-BIPY-Ir	82
	UiO-67-BIPY-Ir	85
2	CAU-27-BIPY-Ir	72
	UiO-67-BIPY-Ir	41
3	CAU-27-BIPY-Ir	48
	UiO-67-BIPY-Ir	20

[a] All reactions were conducted under neat conditions with 0.118 mmol B_2pin_2, 1.250 ml toluene, 1 mol % Ir-catalyst at 100 °C for 24 h.

[b] Yields determined by GC analysis.

In conclusion we discovered two new zirconium terephthalate MOFs, CAU-26 and CAU-27-BDC, utilizing acetic acid as a green and sustainable solvent. CAU-26 crystallizes in a layered structure containing $\{Zr_6O_8\}$ clusters, while CAU-27-BDC exhibits a new IBU, which consists of highly condensed polyhedron-sharing chains of $\{Zr_6O_8\}$ clusters. CAU-26 can be directly transformed into CAU-27-BDC in the mother liquor by increasing reaction temperature and time, while it is also possible to synthesize isoreticular CAU-27-BPDC and CAU-27-BIPY using the extended linker molecules 4,4'-biphenyldicarboxylic acid and 5,5'-dicarboxy-2,2'-bipyridine. It was shown that the iridium-loaded CAU-27-BIPY was a more performant heterogeneous catalyst than the well-known iridium-loaded UiO-67-BIPY for the direct C-H borylation of arenes due to its high thermal and chemical stability. Finally, the possibility to remove or exchange acetate/formate ligands, which are part of the MOF structures, further underlines their potential for other applications, such as ligand attachments, catalysis at open metal sites, pore size tuning, shape selectivity, proton conductivity and many others.

Experimental Section

The supporting information contains a list of the used chemicals, the synthetic and purification procedures for all named compounds, details on the crystal structure determination and characterization methods as well as the results of the latter (electron diffraction, X-ray powder diffraction, thermogravimetric analysis, elemental analysis, ^{1}H NMR experiments, variable temperature diffraction, nitrogen and water adsorption, infrared/RAMAN spectroscopy, stability tests).

[Supporting Information Weblink]

Acknowledgements

Haishuang Zhao greatfully acknowledges the Carl Zeiss Stiftung for the financial support. Lisa Mahnke, Dana Krause, Jan Krahmer, Milan Köppen, Jannik Benecke, Jannick Jacobsen and the spectroscopic section of the department of inorganic chemistry (University of Kiel) is also thanked for their support with various measurements. Niels Van Velthoven, Mickaël Henrion and Dirk E. De Vos thank the NMBP-01-2016 Program of the European Union's Horizon 2020 Framework Program under grant agreement no. [720996] for funding. Niels Van Velthoven and Dirk E. De Vos also thank FWO for funding.

Keywords: Direct C-H borylation • Electron Diffraction • Green Chemistry • Metal-organic Frameworks • Zirconium

[1] M. Taddei, *Coord. Chem. Rev.* **2017**, *343*, 1-24.
[2] P. Couture, C. Blaise, D. Cluis, C. Bastien, *Water, Air, and Soil Pollut.* **1989**, *47*, 87-100.
[3] M. Bosch, M. Zhang, H.-C. Zhou, *Adv. in Chem.* **2014**, 182327.
[4] C. Pettinari, F. Marchetti, N. Mosca, G. Tosi, A. Drozdov, *Polym. Int.* **2017**, *66*, 731-744.
[5] a) N. Bates in *Toxicology of Solvents* (Eds.: M. Mc Parland, N. Bates), Rapra Technology Limited, **2002**, pp. 119-130. b) H. Senoh, S. Aiso, H. Arito, T. Nishizawa, K. Nagano, S. Yamamoto, T. Matsushima, *J. Occup. Health* **2004**, *46*, 429-439. c) D. L. Comis, S. P. Joseph in *e-EROS Encyclopedia of Reagents for Organic Synthesis*, Wiley-VCH, Weinheim, **2001**.
[6] Z. Hu, Y. Peng, Z. Kang, Y. Qian, D. Zhao*, Inorg. Chem.* **2015**, *54*, 4862-4868.
[7] G. Zahn, H. A. Schulze, J. Lippke, S. König, U. Sazama, M. Fröba, P. Beherns, *Micro. Meso. Mater*. **2015**, *203*, 186-194.
[8] H. Reinsch, B. Bueken, F. Vermoortele, U. Stassen, A. Lieb, K.-P. Lillerud, D. De Vos, *Cryst. Eng. Comm.* **2015**, *17*, 4070.
[9] H. Reinsch, S. Waitschat, S. M. Chavan, K.-P. Lillerud, N. Stock, *Eur. J. Inorg. Chem*. **2016**, *27*, 4490-4498,
[10] S. Waitschat, H. Reinsch, N. Stock*, Chem. Commun.* **2016**, *52*, 12698.
[11] A. C. Dreischarf, M. Lammert, N. Stock, H. Reinsch, *Inorg. Chem.* **2017**, *56*, 2270-2277.
[12] S. Waitschat, H. Reinsch, M. Arpacioglu, N. Stock, *Cryst. Eng. Comm.* **2018**, *20*, 5108-5111.
[13] Y. Bai, Y. Dou, L.-H. Xie, W. Rutledge, J.-R. Li, H.-C. Zhou, *Chem. Soc. Rev.* **2016**, *45*, 2327.
[14] J. H. Cavka, S. Jakobsen, U. Olsbye, N. Guillou, C. Lamberti, S. Bordiga, K.-P. Lillerud, *J. Am. Chem. Soc.* **2008**, *130*, 13851.
[15] D. Feng, H.-L. Jiang, Y.-P. Chen, Z.-Y. Gu, Z. Wei, H.-C. Zhou, *Inorg. Chem.* **2013**, *52*, 12661-12667.
[16] a) L. Cooper, N. Guillou, C. Martineau, E. Elkaim, F. Taulelle, C. Serre, T. Devic, *Eur. J. Inorg. Chem.* **2014**, 6281-6289. b) G. Mouchaham, L. Cooper, N. Guillou, C. Martineau, E. Elkaim, S. Bourrelly, P. L. Llewellyn, C. Allain, G. Clavier, C. Serre, T. Devic, *Angew. Chem. Int. Ed.* **2015**, *54*, 13297-13301.
[17] G. Kickelbick, P. Wiede, U. Schubert, *Inorg. Chim. Acta* **1999**, *284*, 1-7.
[18] G. Kickelbick, U. Schubert, *J. Chem. Soc., Dalton Trans*. **1999**, 1301-1305.
[19] G. Kickelbick, U. Schubert, *Chem. Ber./Recueil* **1997**, *130*, 473-477.
[20] M. Puchberger, F. R. Kogler, M. Jupa, S. Gross, H. Fric, G. Kickelbick, U. Schubert, *Eur. J. Inorg. Chem.* **2006**, 3283-3293.

[21] F. R. Kogler, M. Jupa, M. Puchberger, U. Schubert*, J. Mater. Chem.* **2004**, *14*, 3133-3138.

[22] M. J. Cliffe, E. Castillo-Martínez, Y. Wu, J. Lee, A. C. Forse, F. C. N. Firth, P. Z. Moghadam, D. Fairen-Jimenez, M. W. Gaultois, J. A. Hill, O. V. Magdysyuk, B. Slater, A. L. Goodwin, C. P. Grey, *J. Am. Chem. Soc.* **2017**, *139*, 5397-5404.

[23] V. Guillerm, F. Ragon, N. Dan-Hardi, T. Devic, M. Vishnuvarthan, B. Campo, A. Vimont, G. Clet, Q. Yang, G. Maurin, G. Férey, A. Vittadini, S. Gross, C. Serre, *Angew. Chem.* **2012**, *124*, 9401-9405.

[24] U. Kolb, T. Gorelik, C. Kübel, M. T. Otten, D. Hubert, *Ultramicroscopy* **2007**, *107*, 507-513.

[25] U. Kolb, T. Gorelik, M. T. Otten, *Ultramicroscopy* **2008**, *108*, 763-772.

[26] J. Jiang, J. L. Jorda, J. Yu, L. A. Baumes, E. Mugnaioli, M. J. Diaz-Cabanas, U. Kolb, A. Corma, *Science* **2011**, *333*, 1131-1134.

[27] P. Guo, J. Shin, A. G. Greenaway, J. G. Min, J. Su, H. J. Choi, L. Liu, P. A. Cox, S. B. Hong, P. A. Wright, X. Zou, *Nature* **2015**, *524*, 74-78.

[28] H. Zhao, Y. Krysiak, K. Hoffmann, B. Barton, L. Molina-Luna, R. B. Neder, H. J. Kleebe, T. M. Gesing, H. Schneider, R. X. Fischer, U. Kolb, *J. Solid State Chem.* **2017**, *249*, 114-123.

[29] I. Rozhdestvenskaya, E. Mugnaioli, M. Czank, W. Depmeier, U. Kolb, A. Reinholdt, T. Weirich, *Mineral. Mag.* **2016**, *74*, 159-177.

[30] M. B. Mesch, K. Bärwinkel, Y. Krysiak, C. Martineau, F. Taulelle, R. B. Neder, U. Kolb and J. Senker, *Chem. Eur. J.* **2016**, *22*, 16878-16890.

[31] L. Palatinus, P. Brázda, P. Boullay, O. Perez, M. Klementová, S. Petit, V. Eigner, M. Zaarour, S. Mintova, *Science* **2017**, *355*, 166-169.

[32] T. Rhauderwiek, H. Zhao, P. Hirschle, M. Döblinger, B. Bueken, H. Reinsch, D. de Vos, S. Wuttke, U. Kolb, N. Stock, *Chem. Sci.* **2018**, *9*, 5467.

[33] R. Vincent, P. A. Midgley, *Ultramicroscopy* **1994**, *53*, 271-282.

[34] D. Feng, Z.-Y. Gu, J.-R. Li, H.-L. Jiang, Z. Wie, H.-C. Zhou, *Angew. Chem.* **2012**, *124*, 10453-10456.

[35] M. Eddaoudi, J. Kim, N. Rosi, D. Vodak, J. Wachter, M. O'Keeffe, O. M. Yaghi, *Science* **2002**, *295*, 469-472.

Entry for the Table of Contents

COMMUNICATION

New inorganic building unit for zirconium MOFs obtained via green synthesis and revealed by electron diffraction: Zr MOFs with one dimensional chains of highly condensed $\{Zr_6O_8\}$ clusters were obtained upon utilizing acetic acid as a green solvent. The materials exhibit outstanding thermal and chemical stability as well as removable or exchangeable acetate ions.

Sebastian Leubner, Haishuang Zhao, Niels Van Velthoven, Mickaël Henrion, Helge Reinsch, Dirk E. De Vos, Ute Kolb*, Norbert Stock**

Page No. – Page No.

Expanding the Variety of Zirconium-based Inorganic Building Units for Metal-organic Frameworks